



Silver mushroom induced by oxidation in $\text{Cu}_{42}\text{Zr}_{42}\text{Al}_8\text{Ag}_8$ metallic glasses

Ji Liang Zhang*, Wen Huan Cao, Chan Hung Shek

Department of Physics and Materials Science, City University of Hong Kong, Kowloon Tong, Hong Kong, PR China

ARTICLE INFO

Article history:

Received 21 July 2010

Received in revised form

13 December 2010

Accepted 12 January 2011

Available online 21 January 2011

Keywords:

Metallic glasses

Oxidation

TGA

ABSTRACT

The oxidation behavior of $\text{Cu}_{42}\text{Zr}_{42}\text{Al}_8\text{Ag}_8$ metallic glass ribbons at 633–693 K was investigated. The oxidation kinetics followed initially a parabolic rate law but change to a linear one after some time. Mushroom shaped silver crystals were observed on the surface of the oxide layer of the sample oxidized at 663 K and their formation seemed to accelerate the overall oxidation. The formation of the ‘silver mushrooms’ was attributed to the extrusion of silver segregated out during oxidation through weak points in the surface oxide scale. The rounded cap was thought to form due to surface tension or residual stress arising from the extrusion process. Such surface morphology is expected to be beneficial for the metallic glasses as biomaterials.

© 2011 Elsevier B.V. All rights reserved.

1. Introduction

Metallic glasses have been attracting more attentions due to their superior properties for extensive potential applications, such as mirror-like surface for optical components, super-plasticity in supercooled region, good corrosion-resistance, strength approaching theoretical value, superior magnetic properties and good biological properties etc. [1–3]. However there are several factors limiting their scope of applications, especially glass forming ability (GFA) and stability. Over past decades, metallic glasses with high glass forming ability were developed in many systems [4–6]. Among them, Cu–Zr based metallic glasses are popular due to their low materials cost. Cu–Zr binary alloys ($\text{Cu}_{50}\text{Zr}_{50}$ with critical dimension of 2 mm) already show large glass forming ability [7–9]. Minor addition of Al is found to improve the GFA of such alloys effectively, for instance, $\text{Cu}_{42}\text{Zr}_{42}\text{Al}_8$ has a critical radius of 5 mm [10]. Bulk metallic glasses up to centimeters in critical dimension were fabricated by further addition of small amounts of Ag ($\text{Cu}_{42}\text{Zr}_{42}\text{Al}_8\text{Ag}_8$) [11–13]. The properties and structures of Cu–Zr and Cu–Zr–Al metallic glasses were widely studied [14–16]. However, the investigation on properties and structures of Cu–Zr–Al–Ag metallic glasses were seldom reported [17–19]. In this investigation, oxidation of $\text{Cu}_{42}\text{Zr}_{42}\text{Al}_8\text{Ag}_8$ metallic glasses just below glass transition temperature was studied to reveal the thermal stability of such metallic glasses in air. Mushroom-like silver rods were observed on the oxidized surface. It is proposed that the ‘silver mushrooms’ were formed by a mechanism similar to extrusion

through the oxide layer and this process on the surface accelerated the oxidation kinetics.

2. Experimental procedures

$\text{Cu}_{42}\text{Zr}_{42}\text{Al}_8\text{Ag}_8$ alloy ingots were prepared by arc melting the mixtures of pure Cu (99.99 wt.%), Zr (99.9 wt.%), Al (99.99 wt.%) and Ag (99.99 wt.%) metals in a Ti-gettered argon atmosphere. Glassy ribbons with thickness of $\sim 30 \mu\text{m}$ and width of $\sim 2 \text{mm}$ were fabricated by melt-spinning in argon atmosphere. The glass transition temperature and crystallization temperature were measured as 696 K and 775 K, respectively, in a purified nitrogen atmosphere with a Perkin Elmer DSC 7 differential scanning calorimeter (DSC) at a heating rate 20 K/min. Oxidation of melt-spun ribbons were investigated by thermogravimetric analysis (TGA Q50, TA USA) in synthetic air just below glass transition (at 633 K, 663 K and 693 K, respectively, for 3 h). The structure of the oxide scales were studied with a Siemens D 500 diffractometer with $\text{CuK}\alpha$ radiation ($\lambda = 0.15406 \text{nm}$). Surface and cross-section morphologies were observed with JEOL JSM 820 scanning electron microscope (SEM) and JEOL JSM 6335 field-emission SEM. Chemical composition analysis were conducted by energy dispersive X-ray spectrometers (EDX) attached to the two SEMs.

3. Results and discussions

Plots of the mass gain per area with oxidation time are shown in Fig. 1a. It is clear that at all three temperatures the oxidation kinetics of the samples exhibit two distinctive stages after instability of a very short time. Initially, the oxidation obeyed parabolic-rate law, $W = Kt^{1/2}$, and then followed a linear rule $W = Kt$, where W is mass gain per area of the sample, t oxidation time and K is the rate constant. The rate constants and transition time τ at various temperatures were listed in Table 1 (K_1 for the first stage and K_2 for the second stage). From Fig. 1a and Table 1, the sample underwent a fast-growth transient oxidation followed by a slower second stage at 633 K and 693 K. However the sample suffered an accelerated transition when tested at 663 K.

* Corresponding author. Tel.: +852 21942825; fax: +852 27887798.
E-mail address: jiliangz@hotmail.com (J.L. Zhang).

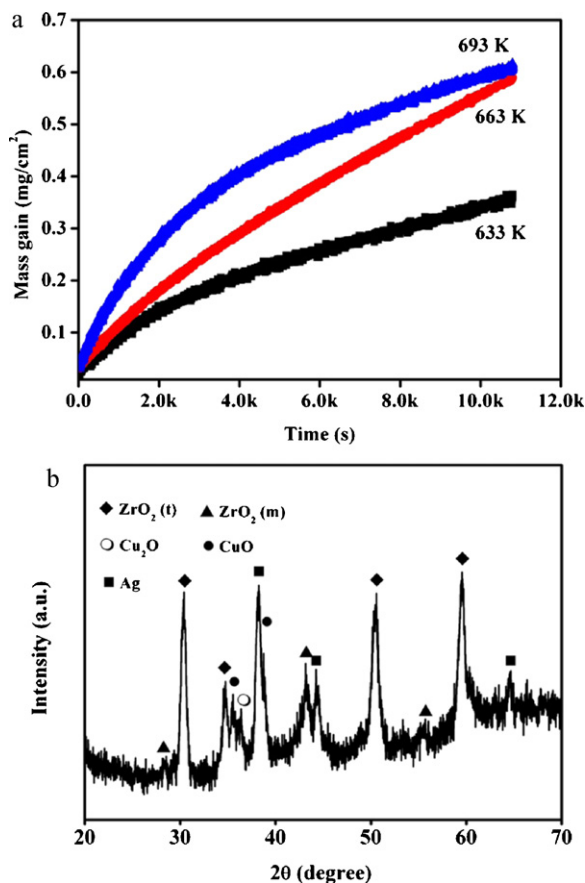


Fig. 1. (a) Plots of mass gain versus time for $\text{Cu}_{42}\text{Zr}_{42}\text{Al}_8\text{Ag}_8$ metallic glass during oxidation tests. (b) XRD pattern of oxide scales obtained at 663 K.

The XRD patterns in Fig. 1b, which is typical for all oxidized samples, indicated that the oxidation scale consisted mostly of tetragonal- ZrO_2 and Ag with minor amounts of CuO and Cu_2O in all samples. The matrix was still amorphous which suggested that the Ag was not produced by pure thermal crystallization of such metallic glass. After oxidation for 3 h at 633 K, oxide scales consisting of two layers were formed. EDX analysis showed that the thin surface layer is CuAg-rich (Cu > 65% and Ag ~ 20%) and the sub-surface layer is Zr-rich. A nearly uniform Cu-rich (Cu > 85%) surface layer also formed at elevated temperature of 693 K after 3 h oxidation, and the content of Ag in the surface is limited (less than 8%). EDX analysis on the cross-section indicated Ag is rich at the bottom of the outer layer.

Close examination of the SEM micrographs of the oxidized surface in Fig. 2a reveals that there are “white” particles on the oxide scale at 663 K. Composition analysis by EDX on more than 10 particles indicated that these particles consist of mainly Ag with minor amount of Cu, and the average composition is given in Table 2. According to Table 2 and the Cu–Ag binary phase diagram [20], it is reasonable to consider these particles as a solid solution of small

Table 1

The rate constants for the oxidation kinetics of the $\text{Cu}_{42}\text{Zr}_{42}\text{Al}_8\text{Ag}_8$ metallic glass at different temperatures. K_1 is for the initial parabolic stage; K_2 for the subsequent stage with linear kinetics and τ is the transition time between the parabolic and the linear stages.

Temp. (K)	K_1 ($\text{g cm}^{-2} \text{s}^{-1/2}$)	K_2 ($\text{g cm}^{-2} \text{s}$)	τ (s)
633	3.60×10^{-6}	2.1×10^{-5}	4600
663	6.10×10^{-6}	4.2×10^{-5}	5300
693	7.20×10^{-6}	2.6×10^{-5}	6800

Table 2

Compositions of different zones on the surface of oxidized samples at 663 K.

Composition	Cu (at.%)	Zr (at.%)	Al (at.%)	Ag (at.%)
Mushroom-like particles	6.8	0	0	93.2
Oxide layer	68.8	11.7	3.5	16
Bulk material	35.7	45.1	10	9.2

amount of Cu in Ag. Close examination of the XRD spectra in Fig. 1b also confirmed that peaks of Ag shifted towards higher diffraction angle, which indicated the decrement in lattice parameters caused by copper solute.

The particles are shown at higher magnification in Fig. 2b and a mushroom-like morphology was revealed. Composition analysis, listed in Table 2, shows that the upper layer of oxide is Cu-rich and the flat base region is Zr-rich compared with the bulk material. Combined with XRD spectra, it can be inferred that the upper layer made up of copper oxides (CuO and Cu_2O) and Ag, and the base mainly consisted of ZrO_2 perhaps with minor amount of copper oxide. The high Ag content in the upper layer is likely to support the growth of these mushrooms.

A cross-sectional secondary electron (SE) image of sample oxidized for 3 h at 663 K is shown in Fig. 2c, which reveals that there are two layers in the surface oxide scale. Results of EDX indicated that the inner scale is Zr-rich and outer scale is loose and Cu-riched, corresponding to the base and upper layer, respectively, in Fig. 2b. Several white precipitates were visible in outer scale as marked by arrows and confirmed as nearly pure silver. Back-scattered electron (BE) image of the cross-section shown in Fig. 2d reveals that there are many such silver precipitates inside the outer oxide scale. Oxidation behaviors around glass transition were generally considered as diffusion-controlled process. However, no mushroom-like precipitate was found in samples annealed for 3 h at 663 K in argon atmosphere, which suggested that the formation of mushroom is not only controlled by diffusion.

In order to understand the structural evolution of Ag precipitates during oxidation, microstructures of samples oxidized for different durations at 663 K were investigated. Fig. 3 presents typical BE image and the corresponding X-ray mapping of constituent elements (Cu, Zr and Ag) of the cross-section of the sample oxidized for 1 h at 663 K. It is clear that the scale contained a thick weakly oxidized layer and a thin strongly oxidized layer, which were both Zr-rich. At top of the scale, Cu oxide and Ag were precipitated. Except for the Ag precipitates, one channel of Ag is also seen to penetrate the oxide layer as marked by the dotted circle in the mapping of Ag (Fig. 3d). Thus a channel structure consisting mainly of oxides and Ag extrusion was formed during oxidation. Similar structures of oxide embedding crystals of alloying element were also found in oxidation of some other metallic glasses [21,22].

According to Cu–Ag [20], Cu–Zr [23] and Ag–Zr [24] binary phase diagrams, the solubility of Ag in Zr is up to 20%, while that of Ag in Cu and Cu in Zr are less than 7%. Thus it is expected that most Ag existed as solute in Zr. During oxidation, Cu was depleted or removed towards sample surface by fast fusion, as indicated by the low Cu content shown in X-rays mapping. Ag was gradually expelled from Zr due to the formation of Zr oxides. The weak boundaries or vacancies induced by oxidation are promising segregation sites for the expelled Ag. The volume expansion by oxidation and thermal expansion both induced compression on the weak regions, thus Ag rod could be extruded out of the sample surface, just like extrusion of Sn whiskers in Pd-free solders [25]. The vacancies left after extrusion of Ag are more promising for the further expulsion of Ag during oxidation due to fast diffusion of Ag at the elevated temperature. Therefore the expelled Ag diffused to the root of Ag rod and pushed it up continuously. Since the temperatures for the oxidation experiments exceeded 50% of the melting of Ag, a low

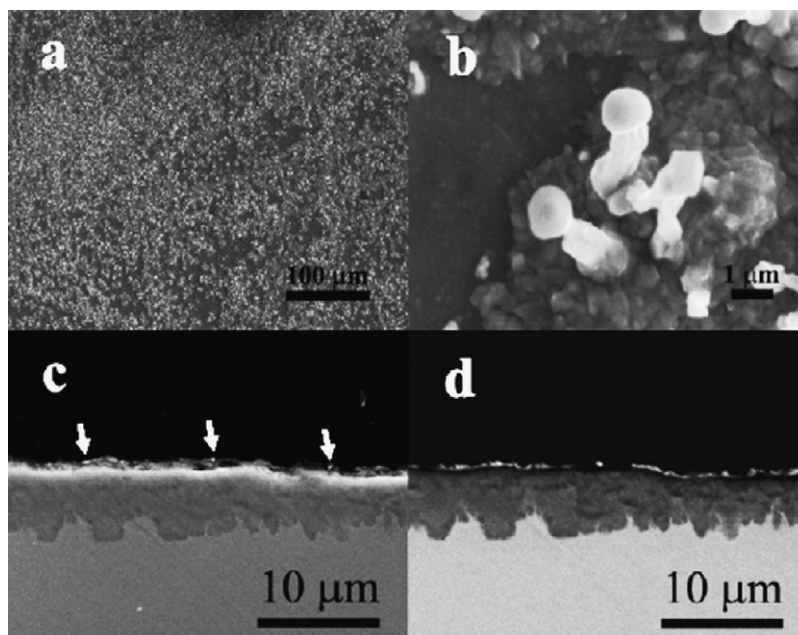


Fig. 2. (a) Surface morphologies of $\text{Cu}_{42}\text{Zr}_{42}\text{Al}_8\text{Ag}_8$ metallic glass oxidized at 663 K; (b) magnified views of the particles in (a); (c) cross-section SE image of samples oxidized at 663 K for 3 h; (d) cross-section BE image of samples oxidized at 663 K for 3 h.

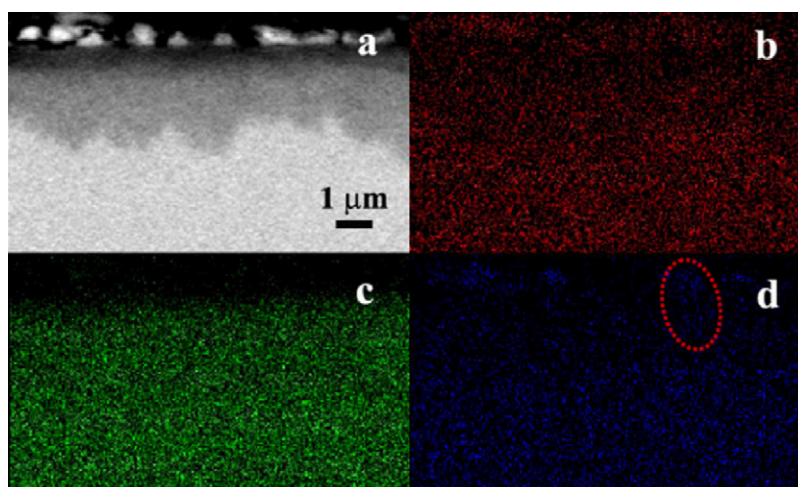


Fig. 3. (a) Cross-section BE image of samples oxidized at 663 K for 1 h and X-ray mapping of elements, (b) Cu, (c) Zr and (d) Ag.

viscosity, or creep strength, of the extruded Ag was expected and the cap of mushroom was likely formed due to creep under the surface tension or residual stress in the extruded Ag. In samples annealed in argon atmosphere, there was no oxide scale and substantial internal stress, thereby no mushroom-like precipitate was observed.

Oxygen diffusion along interface can be orders of magnitude faster than the volume diffusion in the bulk of ZrO_2 grains [22]. Oxidation was therefore accelerated as shown in Fig. 1a. However, since the Zr oxides layer was formed underneath the Cu-rich oxide scale, the extrusion of Ag therefore depends on the thickness of the outer oxide scale. As the temperature increases, a dense and thick Cu oxide outer scale is expected, for instance at 693 K. It seems that the dense layer inhibited the extrusion of silver, because no accelerated oxidation and only scattered mushroom was seen at elevated temperature. However, crack is prone to be initiated due to the interface and the soft Ag, at an elevated temperature.

Summarizing the above discussions, the evolution of silver mushrooms can be illustrated schematically with Fig. 4. At the initial stage of oxidation, some weak regions were produced at the boundary of ZrO_2 and they provided an easy channel for expelling Ag from Zr solid solution. A lamella-like structure was formed during extrusion and accelerated the oxidation. Due to the internal stress and volume expansion induced by the further oxidation,

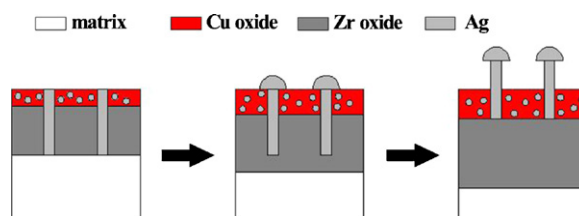


Fig. 4. Schematic illustrations of the formation of Ag mushrooms.

these Ag rods were extruded and cap of mushroom was formed on the surface due to surface tension or residual stress. The continual diffusion of Ag to the weak regions favors the directional growth of the Ag mushrooms.

Having large glass forming ability and being Ni-free, $\text{Cu}_{42}\text{Zr}_{42}\text{Al}_8\text{Ag}_8$ metallic glass may be potential biomaterials. Although the growth of silver mushroom deteriorated the oxidation resistance, it seems to make the metallic glasses more promising in the biomaterials and clinical uses. Due to the wide-spectrum of antimicrobial activity of silver, such extrusion on surface can kill many microbial organisms. Moreover such shape or pattern may benefit anchoring and growth of cell on the surface. Very fine silver (~ 100 nm) precipitates were found in the top layer of oxide scales of $\text{Cu}_{45}\text{Zr}_{45}\text{Al}_5\text{Ag}_5$ metallic glasses [19], which indicated the size of Ag can be controlled for tailored surface properties to suit specific applications.

4. Conclusions

In summary, mushroom of silver solid solution grew on the surface in the oxidation of $\text{Cu}_{42}\text{Zr}_{42}\text{Al}_8\text{Ag}_8$ metallic glass at 663 K. X-rays mapping shows that a lamella-like structure consisting of ZrO_2 embedding Ag rods was formed during oxidation, which also account for the accelerated oxidation at the temperature. After extrusion of Ag rod by further oxidation, a cap formed on the surface. And the mushroom was produced by further extrusion.

Acknowledgement

This work was financially supported by a Strategic Research Grant (Project number 7008101) from City University of Hong Kong.

References

- [1] A.L. Greer, *Science* 267 (1995) 1947.
- [2] W.H. Wang, C. Dong, C.H. Shek, *Mater. Sci. Eng. R* 44 (2004) 45.
- [3] W.L. Johnson, *MRS Bull.* 24 (1999) 42.
- [4] H.S. Chen, *Acta Metall.* 22 (1974) 1505.
- [5] A. Inoue, T. Zhang, T. Masumoto, *Mater. Trans. JIM* 30 (1989) 965.
- [6] A. Peker, W.L. Johnson, *Appl. Phys. Lett.* 63 (1993) 2342.
- [7] M.B. Tang, D.Q. Zhao, M.X. Pan, W.H. Wang, *Chin. Phys. Lett.* 21 (2004) 901.
- [8] A. Inoue, W. Zhang, *Mater. Trans.* 45 (2004) 584.
- [9] D. Xu, B. Lohwongwatana, G. Duan, W.L. Johnson, C. Garland, *Acta Mater.* 52 (2004) 2621.
- [10] P. Yu, H.Y. Bai, M.B. Tang, W.H. Wang, *J. Non-Cryst. Solids* 351 (2005) 1328.
- [11] Q.S. Zhang, W. Zhang, A. Inoue, *Scripta Mater.* 55 (2006) 711.
- [12] Q.S. Zhang, W. Zhang, A. Inoue, *Mater. Trans.* 48 (2007) 629.
- [13] D.S. Sung, O.J. Kwon, E. Fleury, K.B. Kim, J.C. Lee, D.H. Kim, Y.C. Kim, *Metals Mater. Int.* 10 (2004) 575.
- [14] A.J. Kerns, D.E. Polk, R. Ray, B.C. Giessen, *Mater. Sci. Eng.* 38 (1979) 49.
- [15] T.L. Cheung, C.H. Shek, *J. Alloys Compd.* 434 (2007) 71.
- [16] G. Kumar, T. Ohkubo, T. Mukai, K. Hono, *Scripta Mater.* 57 (2007) 173.
- [17] C.L. Qin, W. Zhang, Q.S. Zhang, K. Asami, A. Inoue, *J. Alloys Compd.* 483 (2009) 317.
- [18] J.L. Zhang, J.X. Lu, C.H. Shek, *J. Phys. Conf. Ser.* 144 (2009) 012034.
- [19] W. Kai, I.F. Ren, P.C. Kao, R.F. Wang, C.P. Chuang, M.W. Freels, P.K. Liaw, *Adv. Eng. Mater.* 11 (2009) 380.
- [20] J.L. Murray, *Metall. Trans. A* 15 (1984) 261.
- [21] U. Köster, L. Jastrow, M. Meuris, *Mater. Sci. Eng. A* 165 (2007) 449–451.
- [22] U. Köster, L. Jastrow, *Mater. Sci. Eng. A* 57 (2007) 449–451.
- [23] C.E. Lundin, D.J. McPherson, M. Hansen, *Trans. AIME* 197 (1953) 273.
- [24] J.O. Betterton Jr., D.S. Easton, *Trans. AIME* 212 (1958) 470.
- [25] K. Zeng, K.N. Tu, *Mater. Sci. Eng. R* 38 (2002) 55.